Interseismic Deformation due to Persistent Asperities in Subduction Zones

Eric A. Hetland, Ravi V. S. Kanda, and Mark Simons

I. Abstract

In the last century, several large (M > 7) earthquakes have occured on the megathrust interface along the Japan Trench, offshore of Japan's Tohoku region. Published earthquake source inversions based on seismological data suggest that some of these earthquakes have repeatedly ruptured the same region of the fault (i.e., asperities), while others have ruptured closely clustered asperities (e.g., Yamanaka and Kikuchi, 2004, Panel iV). For instance, the 1978, M 7.4 and the 2005, M 7.2 Miyagi-oki events are inferred to have ruptured the same asperity, while the 1968, M 7.9 Tokachi-oki event, and the 1994, M 7.5 Sanriku-oki event ruptured distinct asperities that are close to each other. In contrast, inversions of geodetic data from interseismic periods produce models that are locked over more spatially extensive regions (e.g., Suwa et al, 2003, Panel IV). These broad and smooth regions are in contrast to the smaller discrete asperities indicated by earthquake source studies, and may be a consequence of lack of model resolution and a resulting need for regularization that is inherent to the use of onshore geodetic data. Alternatively, the differences may imply the potential for a large earthquake in the future. Thus, the different levels of apparent coupling implied by these two classes of models have very different implications for regional seismic hazard. Here, we test the hypothesis that mechanical coupling on inferred asperities alone is sufficient to explain available geodetic observations or alternatively, that these data require additional regions on the megathrust to be coupled. To address this question, we use a 3-D mechanical model of stress-dependent interseismic creep along the megathrust, that is consistent with a given frictional rheology and the known spatio-temporal distribution of large earthquakes (Panel II). These mechanical models predict that asperities are surrounded by a ``halo" of very low creep-rates (a ``stress-shadow" effect) late in the seismic cycle, which also results in a relatively smooth and long wavelength surface velocity field (Panel III). We test if this ``physical" smoothing preserves any signature of the original asperities, in comparison to the artificial smoothing produced by model regularization in inversions of interseismic geodetic data. Underlying this analysis are the assumptions that known asperities persist across multiple earthquake cycles, and that portions of the megathrust that slip co- or post-seismically do not slip interseismically.

II. Methodology & Model Validation

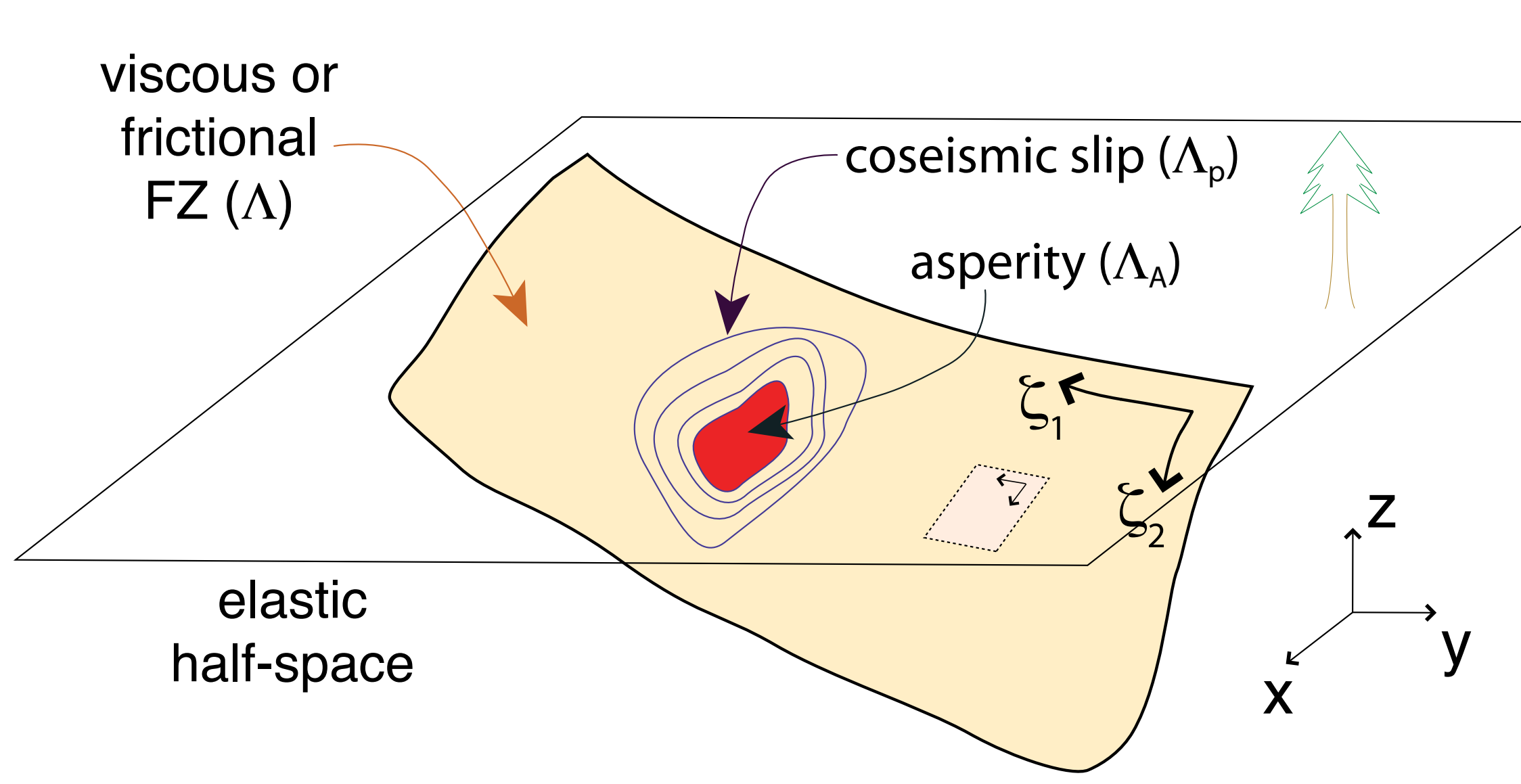

$$\tau_i(\varsigma,t) = \int_{\Lambda}\left[s_j(\xi,t) - tV_j\right]K_{ij}(\varsigma;\xi)d\xi + \sum_p \int_{\Lambda_p} S_{jp}K_{ij}(\varsigma;\xi)d\xi \tag{1}$$

$$f = f_0 + a\ln\left(\frac{v_i}{V_i}\right) + b\ln\left(\frac{v_i\theta_i}{L}\right), \text{ with } \left(\frac{\theta_i}{L}\right) = v_i, \text{ where } v_i = \left(\frac{ds_i}{dt}\right) \tag{2}$$

$$\frac{ds_i(\varsigma,t)}{dt} = \operatorname{sgn}\{\tau_i(\varsigma,t)\}V_i\exp\left\{\frac{|\tau_i(\varsigma,t)| - \sigma_{E_i}(\varsigma)f_0}{(a-b)\sigma_{E_i}(\varsigma)}\right\} = 2V_i\exp\{-\rho_h(\varsigma)\}\sinh\left\{\frac{\tau_i(\varsigma,t)}{\alpha_h(\varsigma)}\right\} \tag{3}$$

Elastic Response Kernels: We first compute the stress and displcement kernels [***K**ᵢⱼ*, in Equation (1)] - which are the elastic responses at the ***i***th observation point (at the surface or over the fault) due to unit slip at the ***j***th fault patch. These kernels depend on the fault geometry, location of the observation points w.r.t. the fault, and the elastic structure of the medium.

Fault Zone Rheology: We next assume a rheology for the fault zone, in order to drive slip evolution on the fault due to the fault tractions in a consistent manner. For modeling the interseismic deformation field, we assume "Hot-friction" [which is equivalent to rate-state friction at steady-state - state variable does not vary with time, as in Equation(2)]. In Panel III, we show that this assumtion is pyhsically reasonable because at times close to the initiation of a megathrust earthquake (i.e., late in the seismic cycle), the elastic fields due to "hot-friction" and rate-state friction are nearly identical.

Numerical Solution Procedure: Starting with some initial conditions, a sequence of earthquakes (periodic/aperiodic) are imposed until the stresses on the fault mature - at which time interseismic creep is no longer dependent on the initial conditions, or the rupture history. Stresses at any time are computed from Equation (1), and Equation (3) is integrated over each seismic cycle until the average fault tractions over the seismic cycle attain a steady-state value, that depends only on the fault rheology and the loading conditions. The time required for this maturation of fault stresses is called "spin-up", and depends on the time taken by imposed stresses (due to fault loading or ruptures) to propagate into the interior of the fault surface. Thus, models with stronger faults, or with greater asperity-boundary distances, will take longer to spin-up. All analysis presented here is for such matured fault interfaces.

Validation Tests: Model Spin-up

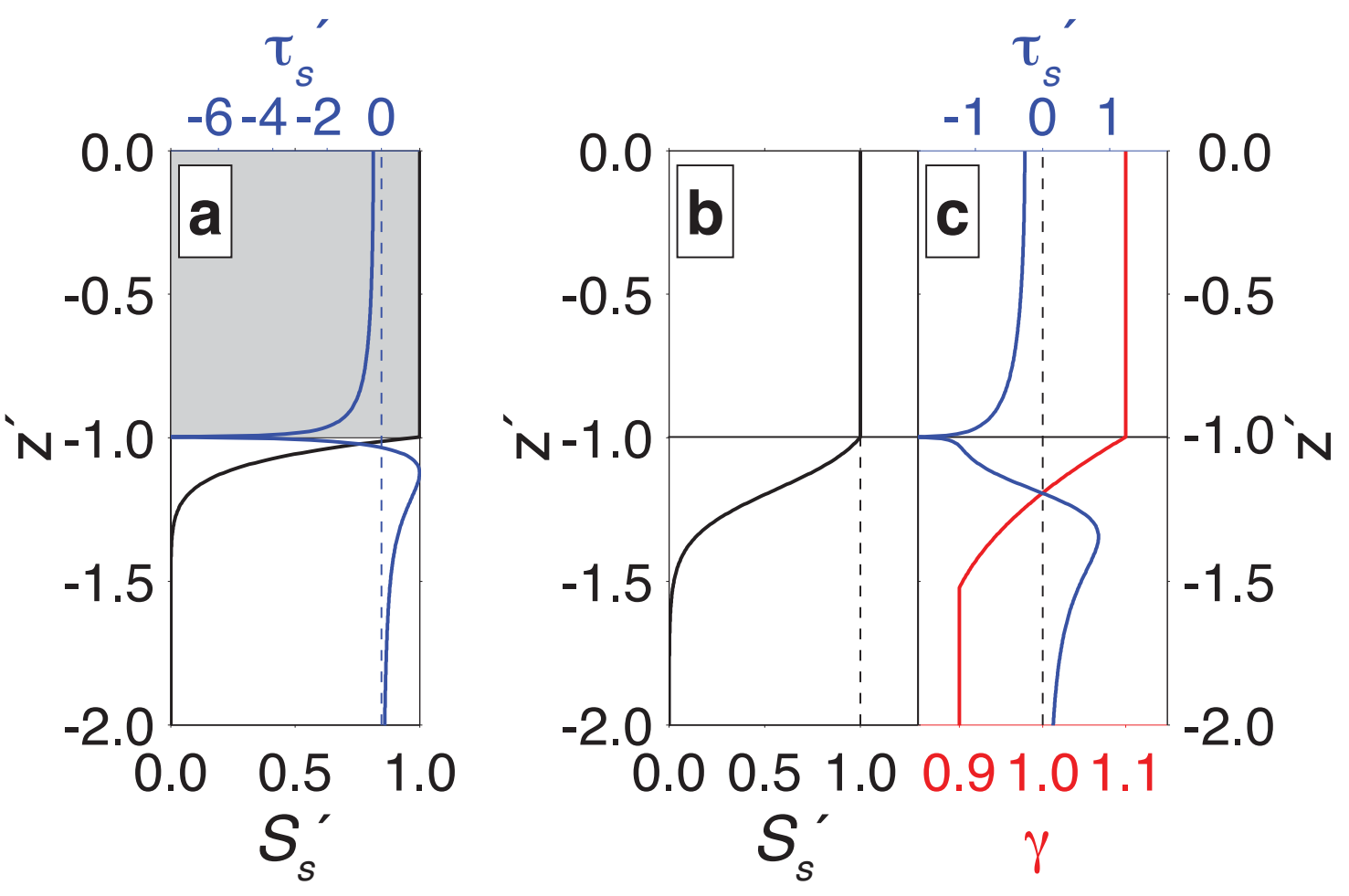

Figure II-1: a) Coseismic slip on a 2D strike-slip fault (S's, black line) and the resulting fault tractions (τ's, blue line); shaded region is locked during the interseismic period. b) Strike-slip rupture (black line) and regions of interseismic fault locking. c) Fault tractions (blue) due to the coseismic slip in (b), and assumed γ (red) in the model in (b).

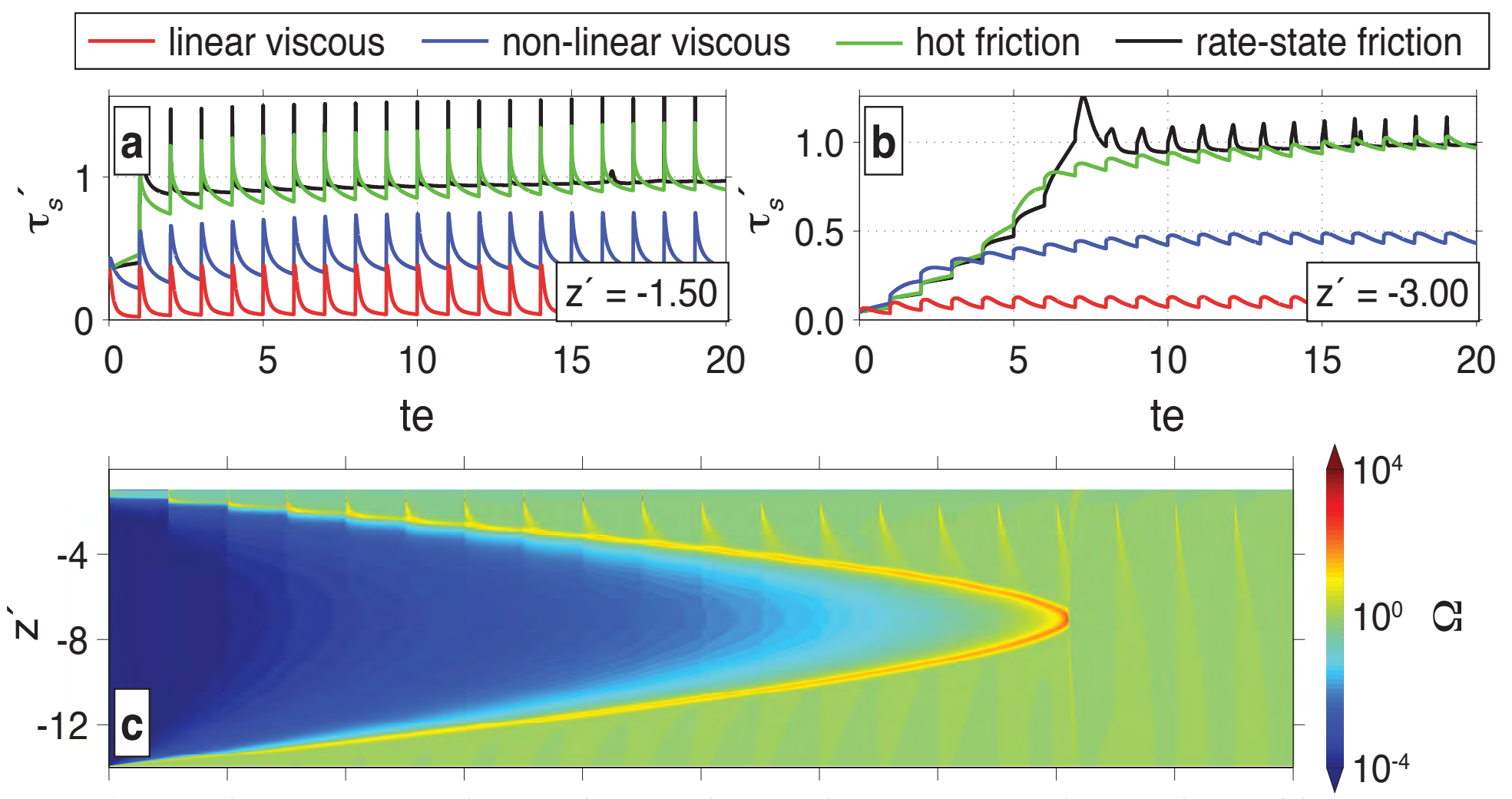

Figure II-2: (a-b) Fault tractions during spin up at z= -1.5D (a) and z = -3.0D (b), in models with linear viscous, non-linear viscous, hot-frictional and rate-state fault rheologies. c) Frictional state variable, θ, during spin-up for rate-state frictional model. Model geometry and rupture slip are shownsn in Figure II-1. **Notice that the state-variable is essentially constant during the later part of the seismic cycle once the fault matures, and is relatively uniform throughout the cycle, away from the location of the asperities themselves.**

Validation Tests: Boundary Effects

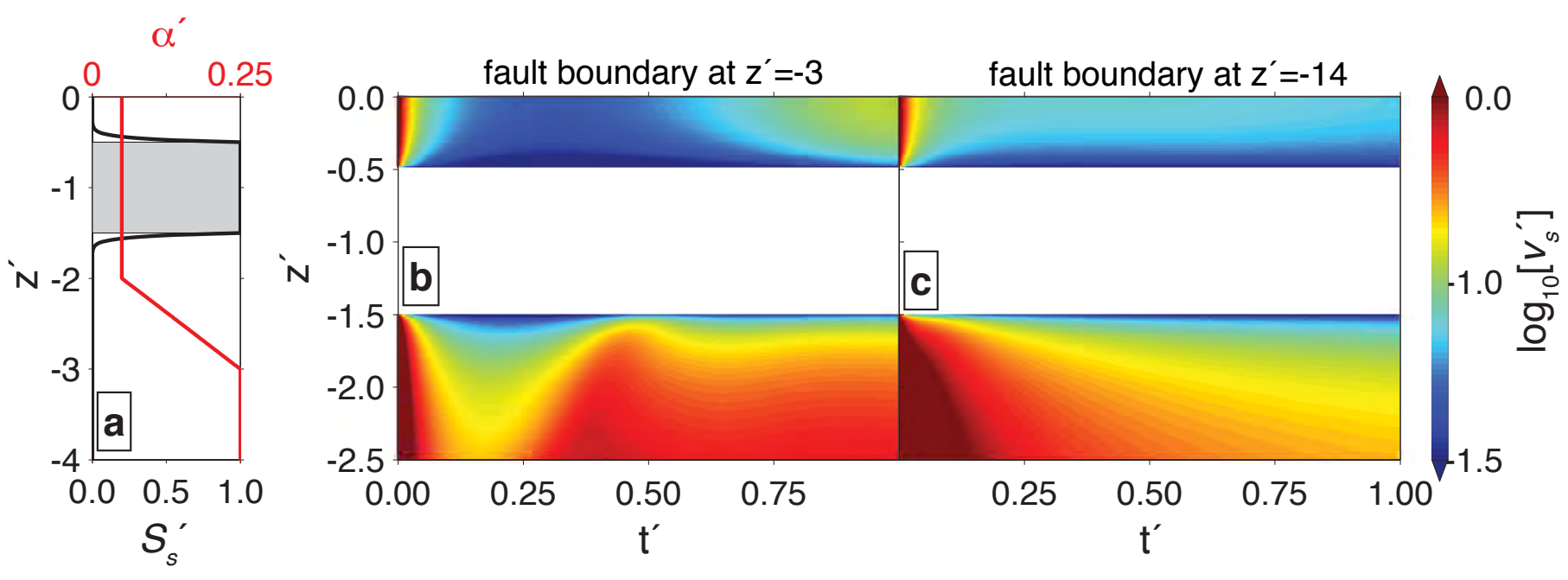

Figure II-3: a) Coseismic slip (black), and strength parameter, α' (red) in a 2D vertical strike-slip fault model with a rate-state friction fault (same parameters as in Figure II-2); shaded area is the locked portion of the fault. b and c) Mature interseismic creep rate in a model with a lower fault boundary at z'= -3 (b) and z'= -14 (c). Notice that when the bottom boundary is too close to the bottom of the locked patch, the boundary conditions cause a faster decay of creep above and below the locked zone, and a subsequent creep pulse that lasts for the remainder of the seismic cycle on either side of the locked zone. On the other hand, when the boundary is far away, then the **creep rates decay during the seismic cycle resulting in an area larger than the locked zone having negligible creep before the next earthquake.**

III. Model Predictions for the Interseismic

Justification for hot-friction fault rheology to model interseismic deformation

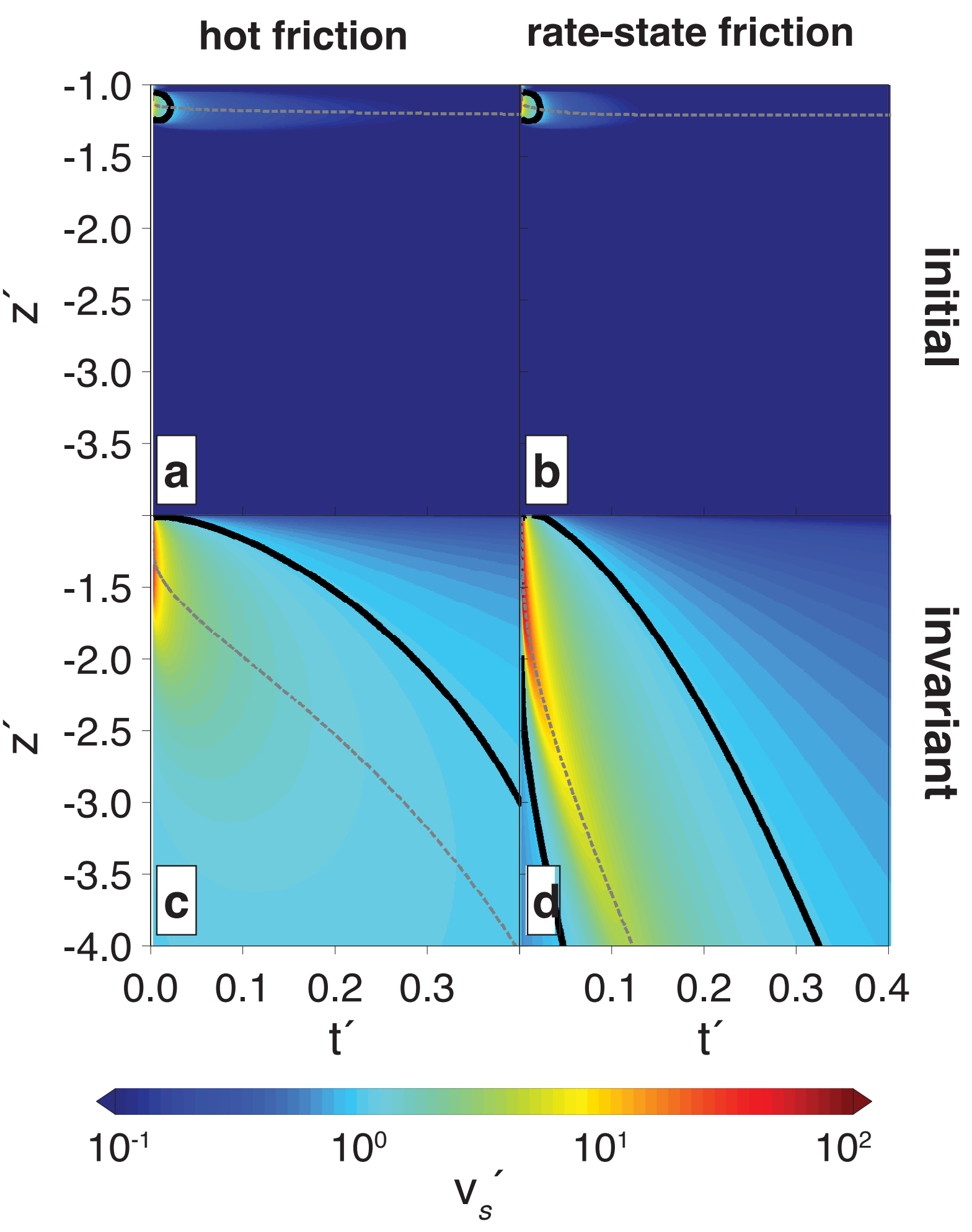

Figure III-1: Fault creep rate in the hot-friction and rate-state models depicted in Figure 11-2 (strike-slip fault), during the initial (a-b), and mature (c-d) seismic cycles. Black solid lines are the vs'= 1 isovelocity contours (i.e., plate rate), and the dotten lines indicate the depth of the maximum creep rate at each time. Note that beyond t' = 0.4, the creep rates both on and off the fault for both models are very similar, and become nearly identical, closer to the next earthquake (t'=1, not shown here).

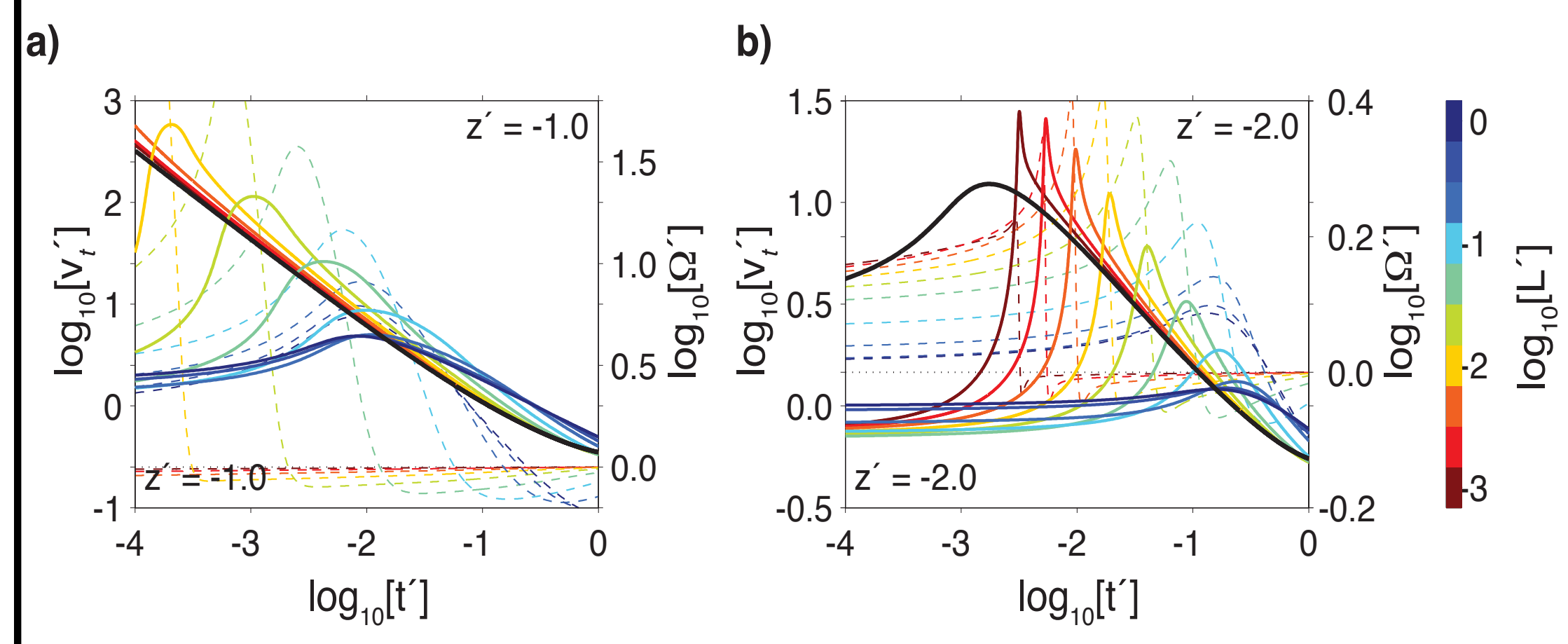

Figure III-2: Cycle invariant creep rates in hot-friction (black line) and rate-state friction faults (solid colored lines, with dimensionless decay length scale, L' given by the color scale). Also shows is the dimensionless state variable, Ω, in the rate-state fault models. Note that for L',= 0.01, and times > 0.1t' (t' = 1 is the full earthquake cycle), both hot-friction and rate-state predictions of cycle invariant creep rates are nearly identical to each other.

Subduction Megathrust Shadow Zones during the Interseismic Period

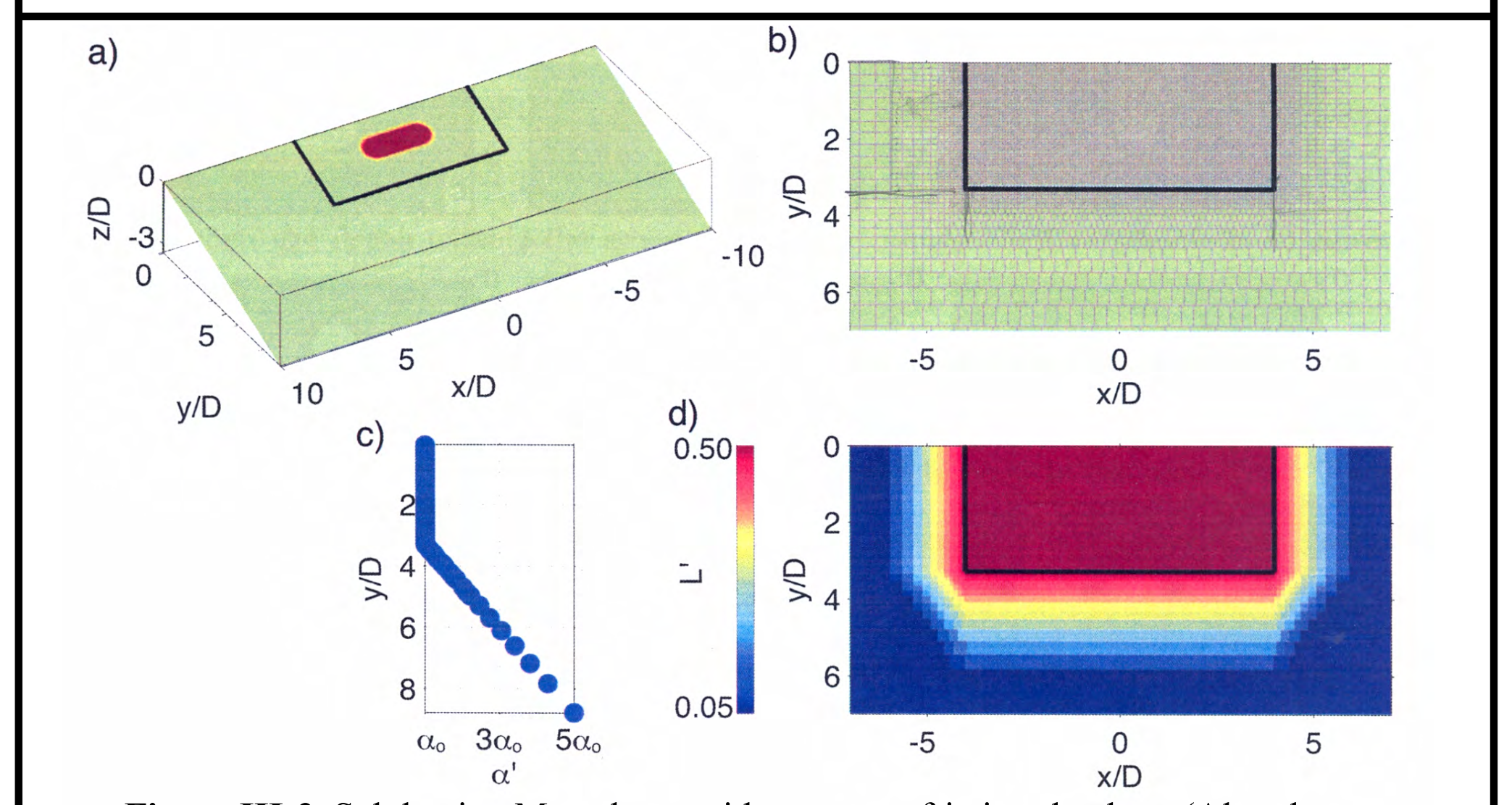

Figure III-3. Subduction Megathrust with rate-state friction rheology (Also shown are the numerical mesh and distribution of rate-state friction parameters)

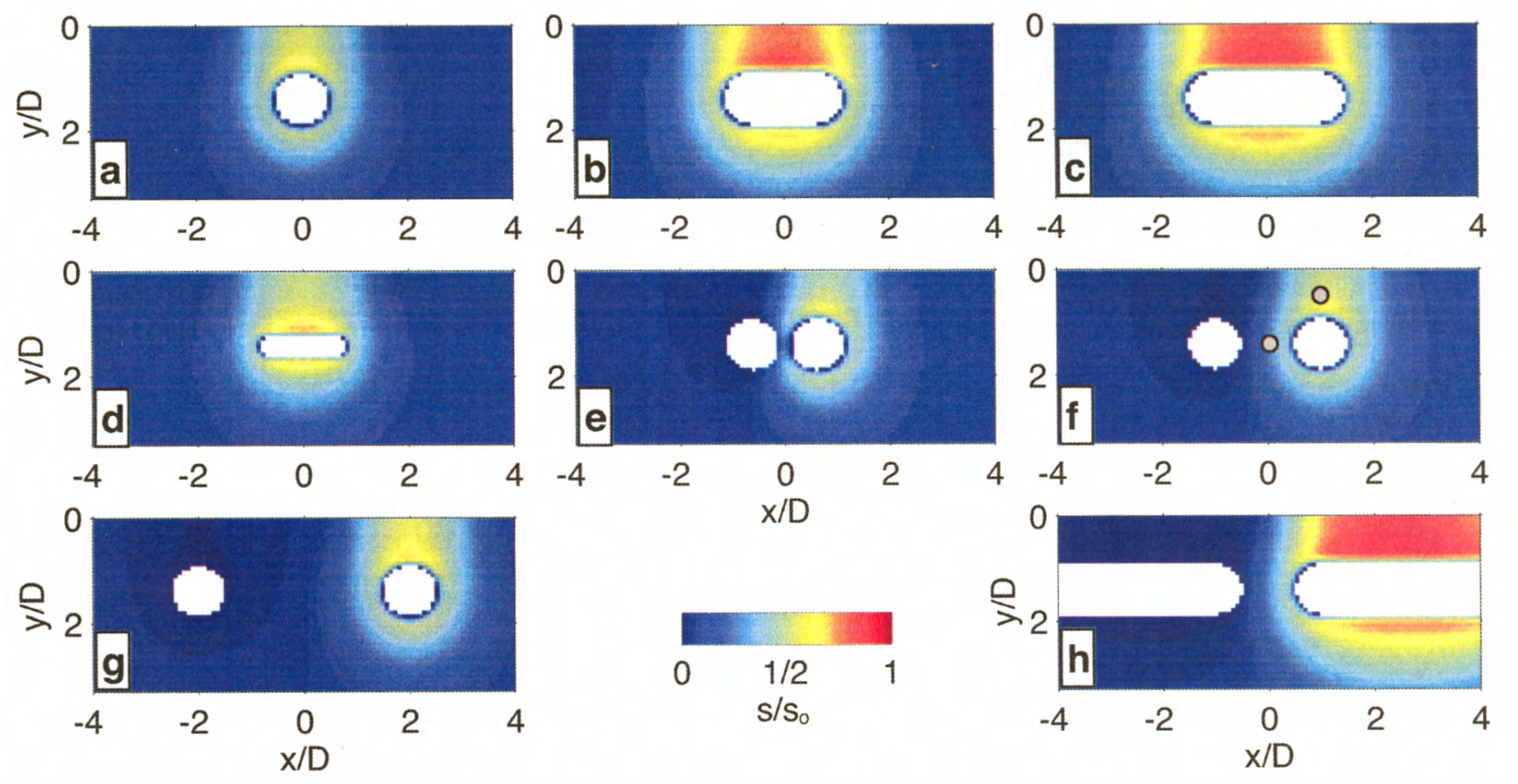

Figure III-4. Immediate post-seismic (t' = 0.05) creep on the megathrust mostly occurs updip of the locked patches, as observed in Sumatra by Hsu et al (Science 2005).

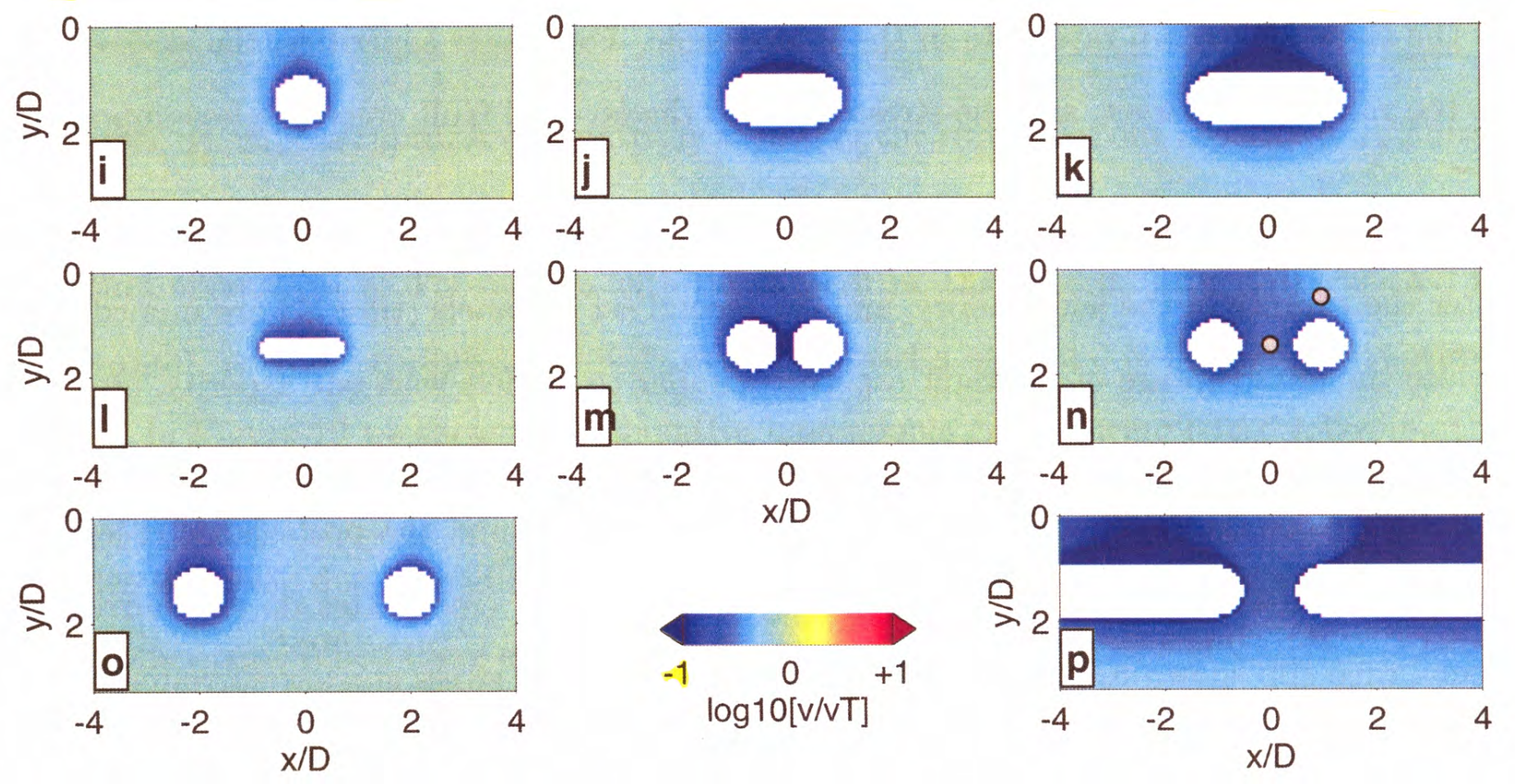

Figure III-5. Interseismic (t' ~ 1.0) creep is negligible in the regions that experienced co- and post-seismic slip.

The regions of the megathrust experiencing rapid post-seismic creep also experience interseismic creep rates that are well below the plate loading rate - these are regions experiencing a "stress-shadow" effect late in the seismic cycle. As a result, there is a larger region of the fault - compared to the original asperities that ruptured - which would appear to be geodetically coupled.

IV. Future Work: Application to Japan

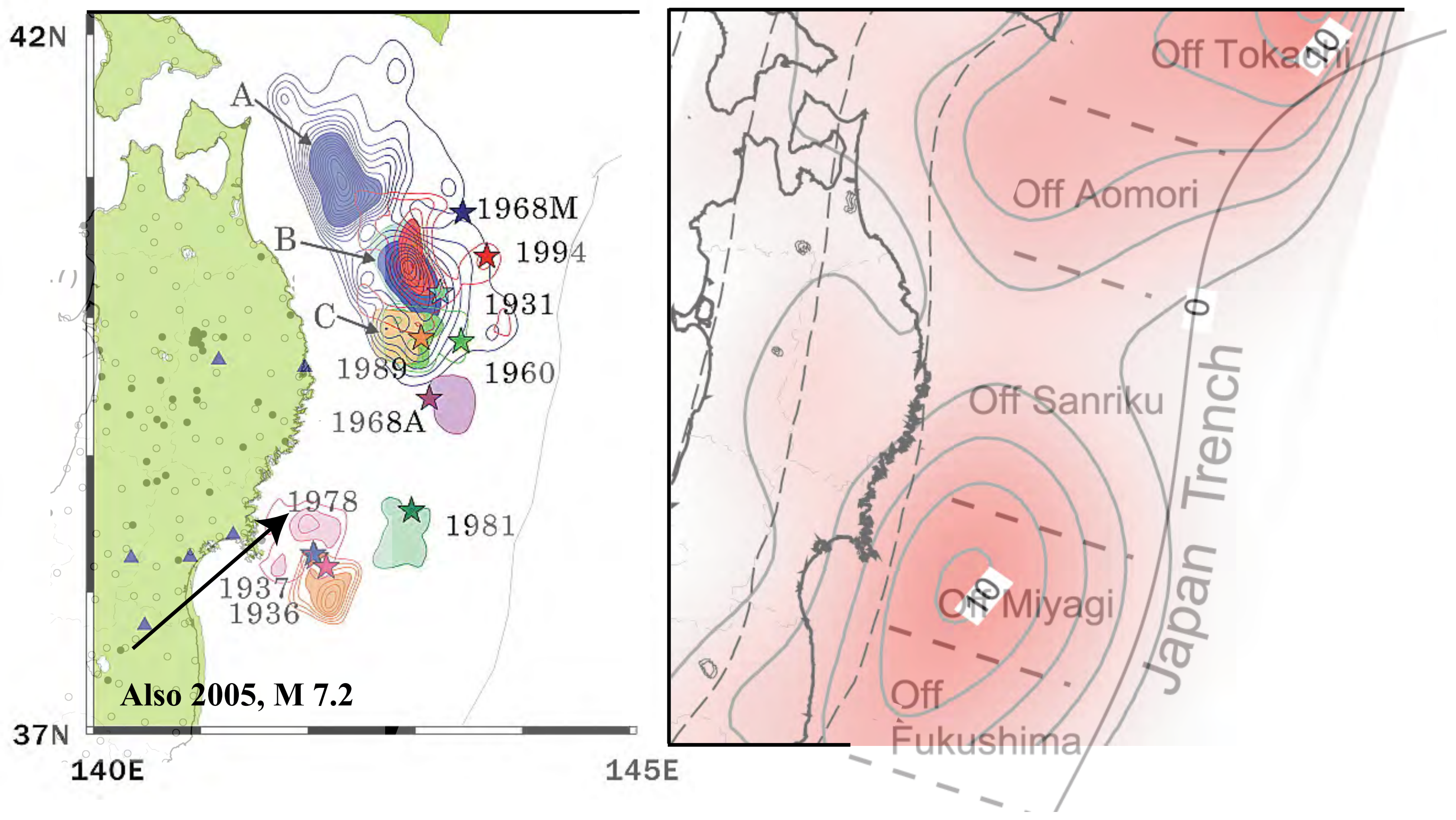

(a) Seismic Source Inversions (Adapted from Yamanaka & Kikuchi, JGR 2004)

(b) Interseismic Geodetic Data (backslip) Inversion (Adapted from Suwa et al., JGR 2006)

Figure IV. Slip estimates for the megathrust interface off (Tohoku) northeastern Japan over the seismic cycle.

Asperities inferred from seismic source inversions tend to be much smaller than the inferred zone of coupling from surface geodetic data (open circles in leftmost figure show locations of geodetic stations). Our goal is to estimate (a) how much of the present interseismic geodetic signal in Tohoku (northeastern Japan) can be explained by coseismic slip only along the asperities for the sequence of M>7 earthquakes (Fig IVa) that occured this century, and (b) whether postseismic slip on the megathrust interface outside of those asperities (as in the above "hot-friction" examples) is required by the interseismic geodetic data (as in the numerically regularized backslip in Fig IVb).